Cage Compounds Hot Paper

How to cite: *Angew. Chem. Int. Ed.* **2022,** *61,* e202201700
International Edition: doi.org/10.1002/anie.202201700
German Edition: doi.org/10.1002/ange.202201700

Heterotrimetallic Double Cavity Cages: Syntheses and Selective Guest Binding

*Lynn S. Lisboa, Dan Preston, C. John McAdam, L. James Wright, Christian G. Hartinger, and James D. Crowley**

Abstract: A strategy for the generation of heterotrimetallic double cavity (DC) cages $[Pd_nPt_mL_4]^{6+}$ (**DC1**: $n=1$, $m=2$; and **DC2**: $n=2$, $m=1$) is reported. The DC cages were generated by combining an inert platinum(II) tetrapyridylaldehyde complex with a suitably substituted pyridylamine and Pd^{II} ions. ^1H and DOSY nuclear magnetic resonance spectroscopy (NMR) and electrospray ionization mass spectrometry (ESIMS) data were consistent with the formation of the DC architectures. **DC1** and **DC2** were shown to interact with several different guest molecules. The structure of **DC1**, which features two identical cavities, binding two 2,6-diaminoanthraquinone (**DAQ**) guest molecules was determined by single-crystal X-ray crystallography. In addition, **DC1** was shown to bind two molecules of 5-fluorouracil (**5-FU**) in a statistical (non-cooperative) manner. In contrast, **DC2**, which features two different cage cavities, was found to interact with two different guests, **5-FU** and **cisplatin**, selectively.

Introduction

Nature exploits self-assembled architectures (DNA, RNA, proteins and virus capsids) in a myriad of important biological processes. Inspired by this, metallosupramolecular chemists have developed a vast range of increasingly larger, self-assembled metal–organic cages (MOCs)[1] and a wide variety of potential applications of these systems have emerged.[2] However, the majority of MOCs studied to date are of very high symmetry and there has been a push recently towards developing lower symmetry systems in order to attain enhanced functionally. In addition to targeting cages with lower symmetry,[3] including heterobimetallic cage systems,[4] there has also been a surge of interest in developing MOCs that feature more than one cavity,[5] as the compartmentalization of molecular recognition events[6] could potentially lead to new applications. Several multicavity MOCs[5] have been developed but the most common examples are constructed using palladium(II) ions as the metal component. Double-[7] $[Pd_3L_4]^{6+}$, triple-[8] $[Pd_4L_4]^{8+}$ and even quadruple-[9] $[Pd_6L_6]^{12+}$ cavity systems have been generated.[10] In addition to these systems there are several mechanically interlocked Pd^{II}-based MOCs that also display multiple cavities.[11] The molecular recognition properties of some of these systems have been examined and, in some cases, segregated binding of two different types of guests has been achieved.[7c,8,12] However, these impressive results have all been generated with homometallic systems.

Herein, building on our recent work that developed heterobimetallic $[PdPtL_4]^{4+}$ cages,[13] we describe a method for the assembly of heterotrimetallic double cavity cages $[Pd_nPt_mL_4]^{6+}$ (**DC1**: $n=1$, $m=2$; and **DC2**: $n=2$, $m=1$) (Figure 1). In addition, we report the host–guest chemistry of these systems with several different neutral guest molecules.

Results and Discussion

We set out with the idea to further develop the conditions we used previously to generate a mono-cavity $[PdPtL_4]^{4+}$ cage (**MC**),[13] with the goal of synthesizing two new heterotrimetallic double cavity cages $[Pd_nPt_mL_4]^{6+}$ (**DC1**: $n=1$, $m=2$ and **DC2**: $n=2$, $m=1$; Figure 1 and Scheme 1). The required substituted pyridylamine linker precursors (**L1** and **L2**, Scheme 1) were synthesized in modest yields (36–41 %) using Pd-catalyzed Sonogashira[15] cross-coupling methods (Supporting Information, Scheme S1 and S2).[8,14a,16]

We reasoned that combining the inert platinum(II) tetrapyridylaldehyde complex, $\mathbf{Pt_{pyald}}$, with a suitably substituted pyridylamine and $[Pd(CH_3CN)_4](BF_4)_2$ in $[D_6]$DMSO should then lead to the assembly of the two double cavity cages **DC1** and **DC2** (Scheme 1). $\mathbf{Pt_{pyald}}$ (2 eq.), $[Pd(CH_3CN)_4](BF_4)_2$ (1 eq.) and **L1** (4 eq.) were combined in $[D_6]$DMSO at room temperature (RT) and the reaction was monitored using ^1H NMR spectroscopy

[*] L. S. Lisboa, Dr. C. J. McAdam, Prof. J. D. Crowley
Department of Chemistry, University of Otago,
PO Box 56, Dunedin 9054 (New Zealand)
E-mail: jcrowley@chemistry.otago.ac.nz
Dr. D. Preston
Research School of Chemistry, Australian National University,
Canberra ACT 0200 (Australia)
Prof. L. J. Wright, Prof. C. G. Hartinger
School of Chemical Sciences, University of Auckland,
Private Bag 92019, Auckland 1142 (New Zealand)

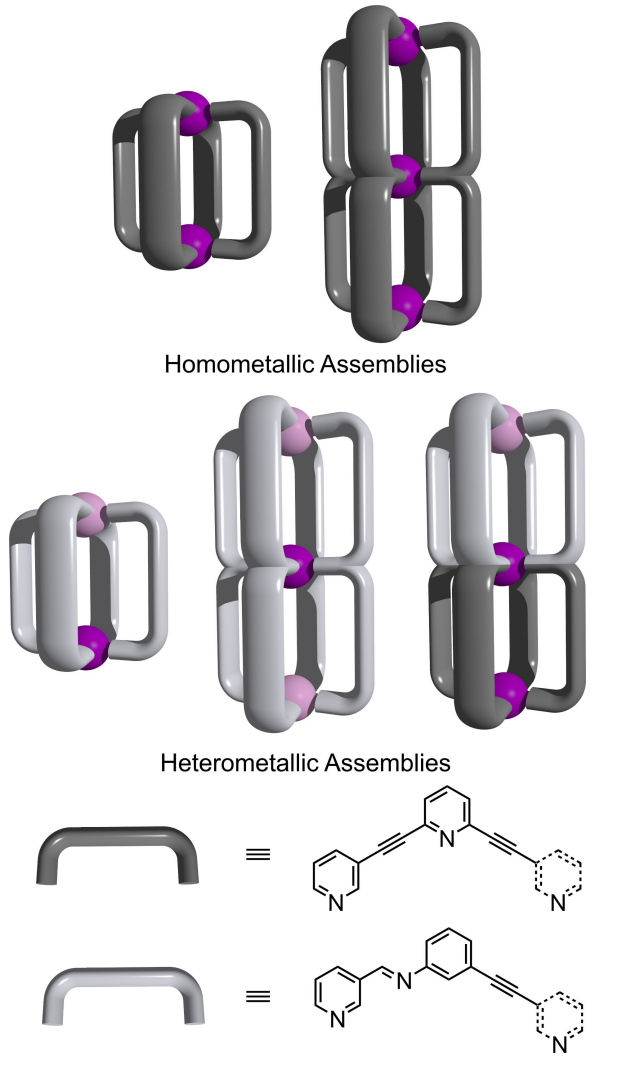

Figure 1. Cartoon representations of homometallic $[Pd_2(L_{tripy})_4]^{4+}$ (top left) and the related $[Pd_3L_4]^{6+}$ double cavity (top right) cages. Bottom: A lower symmetry heterobimetallic $[PdPtL_4]^{4+}$ cage[13] (left) along with heterotrimetallic $[PdPt_2L_4]^{6+}$ (middle) and $[Pd_2PtL_4]^{6+}$ double cavity (right) cages. Colors: palladium(II) = purple, platinum(II) = pink, grey and light grey = semi rigid linker ligands. L_{tripy} = 2,6-bis(pyridin-3-ylethynyl)pyridine.[14]

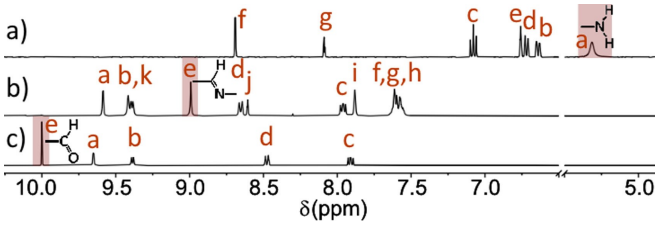

Figure 2. Stacked partial ^{1}H NMR spectra (400 MHz, [D_6]DMSO, 298 K) of a) linker precursor **L1**, b) double cavity cage **DC1**, and c) platinum(II) tetrapyridylaldehyde complex $\mathbf{Pt_{pyald}}$. The proton labels correspond to those shown in Scheme 1.

(Scheme 1, Figures 1 and 2, and Supporting Information). After 5.5 h, the signals (Figures 2a,c) of the $\mathbf{Pt_{pyald}}$ complex and the diamine **L1** had completely disappeared and were replaced by a new series of resonances (Figure 2b). Diagnostic of cage formation, the aldehyde and amine resonances of **L1** and $\mathbf{Pt_{pyald}}$, respectively, were replaced by a signal (H_i, $\delta = 8.99$ ppm) consistent with imine formation and the α-pyridyl peaks (H_a and H_b) were shifted downfield, relative to **L1**, indicating coordination to the Pd^{II} ion. This behavior mirrored what was observed for the related heterobimetallic cage **MC**.[13] However, the assembly of the **DC1** system proceeded more slowly (5.5 h *cf.* 1 h).

The second double cavity cage **DC2** featuring two different cavities could be generated under similar conditions. Combining $\mathbf{Pt_{pyald}}$ (1 eq.), $[Pd(CH_3CN)_4](BF_4)_2$ (2 eq.) and **L2** (4 eq.) in [D_6]DMSO at RT slowly led to the formation of **DC2** over 7 d. The reaction was repeated at 50 °C and after 10 h ^{1}H NMR spectroscopy indicated the assembly of **DC2** being complete with no resonances for the starting material observed and a new imine signal present at $\delta = 8.96$ ppm (Supporting Information). Although these NMR experiments provided no indication that any products other than the new cage systems **DC1** or **DC2** were formed in these reactions, the isolation and purification procedure adopted indicated small amounts of by-products were also formed. Thus, addition of ethyl acetate to the DMSO solutions of the initially synthesized **DC** cages led to the precipitation of colorless or tan solids in high yields (87 or 95 %). Subsequent addition of acetonitrile to these solids resulted in selective dissolution of the cages **DC1** or **DC2**, leaving small amounts of insoluble colorless by-products behind in each case.

To obtain further insight into these assembly reactions we repeated the syntheses of **DC1** and **DC2** in the presence of an internal standard (*tert*-butanol, Supporting Information). As with the initial assembly experiments the starting materials were completely consumed after 5.5 or 10 h, for **DC1** and **DC2**, respectively, and only proton signals due to the cages could be seen. However, integration of the cage signals versus those of the *tert*-butanol internal standard suggested that the cages were generated in 63 (**DC1**) and 79 % (**DC2**) yield, respectively. This indicated that there must be other species present, that are not observed in the NMR spectra, that account for the rest of the starting materials. Given that all the starting materials were consumed during the reaction we postulated that the by-products could be oligomeric/polymeric materials with very broad NMR resonances. However, these by-products can be removed using the method described above to obtain pure samples of the DC cages.

The purified cages **DC1** and **DC2** were analyzed and characterized using ^{1}H, and ^{1}H DOSY NMR, HPLC and ESIMS (Supporting Information). The ^{1}H NMR spectra of the acetonitrile-soluble fractions of **DC1** and **DC2** in CD_3CN were very similar to the spectra observed in [D_6]DMSO. In both cases, the ^{1}H DOSY NMR spectra (CD_3CN, 298 K) showed that all the proton resonances within the individual samples had the same diffusion coefficients ($D_{DC1} = 4.50 \times 10^{-10}$ m^{2}s^{-1} and $D_{DC2} = 4.55 \times 10^{-10}$ m^{2}s^{-1}), suggesting forma-

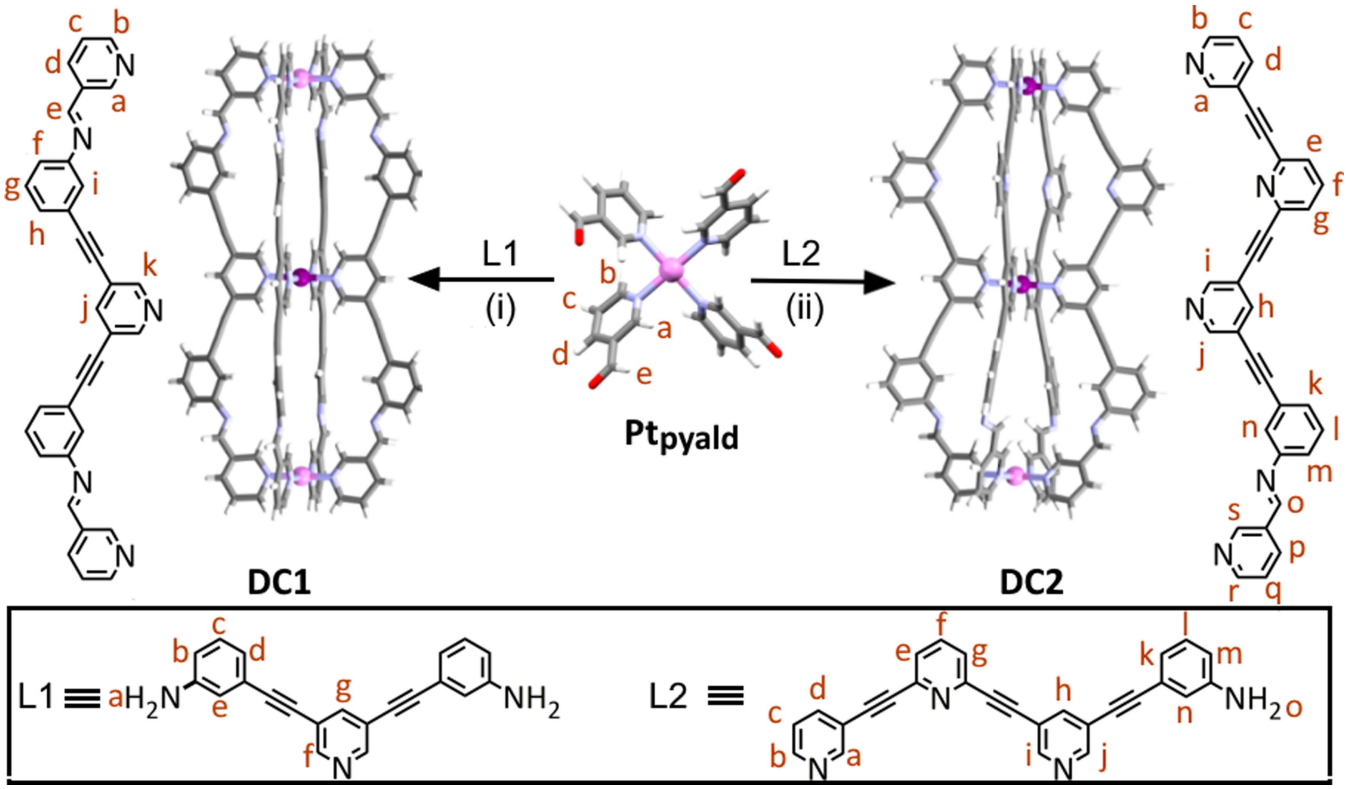

Scheme 1. Synthesis of the double cavity cages **DC1** ($[PdPt_2L_4](BF_4)_6$) and **DC2** $[Pd_2PtL_4](BF_4)_6$: **DC1**: i) $\mathbf{Pt_{pyald}}$ (2 eq.), **L1** (4 eq.), and $[Pd(CH_3CN)_4](BF_4)_2$ (1 eq.), $[D_6]$DMSO, RT, 5.5 h; **DC2**: ii) $\mathbf{Pt_{pyald}}$ (1 eq.), **L2** (4 eq.), and $[Pd(CH_3CN)_4](BF_4)_2$ (2 eq.), $[D_6]$DMSO, 50 °C, 10 h. The tube structures of **DC1** and **DC2** were generated using SPARTAN'16® (MMFF models). The molecular models indicated the cages are similar in size/length, the Pt–Pt distance for **DC1** was 22.88 Å and the Pd–Pt distance 11.44 Å, while the end-to-end Pt–Pd distance for **DC2** was 23.23 Å, the end-to-middle Pd–Pt distance 11.40 Å and the Pd–Pd distance 11.83 Å. Color: pink = platinum, purple = palladium, light blue = nitrogen, red = oxygen, grey = carbon, white = hydrogen.

tion of a single product (Supporting Information, Figures S24 and S25, and Table S1).

Additionally, the diffusion coefficients for **DC1** and **DC2** were very nearly identical and consistent with the formation of two cage molecules of similar molecular size and shape. Furthermore, the diffusion coefficients of **DC1** and **DC2** were different to those found for **L1**, **MC** and $\mathbf{Pt_{pyald}}$ and consistent with the formation of the larger double cavity architectures (Supporting Information, Table S1). ESIMS data obtained from the acetonitrile solutions were also consistent with the formation of the cages **DC1** and **DC2**. For example, the ESIMS data for **DC1** featured several major isotopically resolved peaks observed at $m/z = 496.3036$ $[PdPt_2(\mathbf{L1})_4(Cl)]^{5+}$, 629.1223 $[PdPt_2L_4(Cl)_2]^{4+}$, 642.1310 $[PdPt_2L_4(Cl)(BF_4)]^{4+}$ and 885.1754 $[PdPt_2L_4(Cl)(BF_4)_2]^{3+}$ consistent with the presence of the $[PdPt_2(\mathbf{L1})_4]^{6+}$ cage (Supporting Information, Figure S16). HPLC (CH_3CN, C18) chromatograms of **DC1** and **DC2** showed that the samples only contained one compound. Additionally, the retention times of the DC cages were different to the related **MC** system and the cage precursors **L1** and $\mathbf{Pt_{pyald}}$, providing further evidence for the formation of the new DC architectures (Supporting Information, Figure S28).

Having developed a robust method for the synthesis and purification of heterotrimetallic DCs, we next investigated the host–guest chemistry of the systems. We had previously shown that the related heterobimetallic cage (**MC**) would interact strongly with 2,6-diaminoanthraquinone (**DAQ**).[13] Therefore, we initially examined the host–guest chemistry of **DC1** and **DC2** with this guest molecule. The signals in the ^{1}H NMR spectra ($[D_6]$DMSO, 298 K) of host–guest mixtures were broad but clearly displayed large complexation-induced shifts indicative of guest binding (Supporting Information, Figures S33 and S34). The NMR spectra obtained for the **MC**:**DAQ** host–guest system[13] displayed slow exchange on the NMR time scale and suggested that the **DC** host–guest adducts behaved similarly. However, interpretation of the NMR data was complicated because the peaks were broadened and/or overlapped. Most likely this was caused by the presence of both 1:1 and 1:2 host–guest adducts. However, this was potentially also due to different respective orientations of the two bound guests relative to one another. The ESIMS data (Supporting Information Figure S35 and S36) obtained from the host–guest mixtures confirmed the formation of the host–guest complexes with spectra displaying peaks due to both 1:1 and 1:2 adducts, for example $m/z = 554.3263$ $[\mathbf{DC1}:\mathbf{DAQ}\text{-}(BF_4)]^{5+}$ and 601.9412 $[\mathbf{DC1}:\mathbf{2DAQ}(BF_4)]^{5+}$ (Supporting Information). Ultimately, the molecular structure of the **DC1**:**2DAQ** host–guest complex was determined using

single crystal X-ray crystallography (Figure 3 and Supporting Information).[17]

Single crystals of the **DC1**:**2DAQ** host–guest adduct were grown by slow vapor diffusion of ethyl acetate into a DMSO solution containing a 1:2 host–guest mixture. The X-ray structure confirmed the formation of the double cavity architecture with Pd^{II} coordinated to the central pyridyl moiety and Pt^{II} coordinated to the two pyridylimine ends. The crystallographically determined Pt1–Pt1′ 23.466(2) Å and Pt1–Pd1 11.733(2) Å distances correspond well with those determined by molecular modelling (Scheme 1 and Supporting Information). Unsurprisingly, the two cavities of **DC1** were of a similar size to that of the analogous $[PdPtL_4]^{4+}$ monocavity cage host–guest adduct with Pd–Pt distances of ≈11.73 Å. Each cavity of the **DC1** architecture contained a **DAQ** guest molecule and, as was observed previously with the monocavity architecture,[13] hydrogen-bonding interactions between the carbonyl groups of the guest and the acidic α-pyridyl hydrogens of the cage stabilized the host–guest interaction (Figure 3 and Supporting Information).

Due to the complicated NMR spectra with overlapping peaks, we were not able to carry out a titration to determine the binding constants for the **DC1-DAQ** interaction so we examined other guests in order to identify one that did not have this problem. When the known anti-cancer drug 5-fluorouracil (**5-FU**) was added to either the **MC** or **DC** cages, small complexation-induced shifts ($\Delta\delta = 0.07$–0.13 ppm) were observed for the *endo* α-pyridyl hydrogen resonances that line the Pd–Pt cavities of the metallo-architectures (Supporting Information). This suggested that **5-FU** was bound within the cage cavities. ESIMS data obtained for the cage:**5-FU** mixtures displayed peaks consistent with the formation of 1:1 host–guest adducts in the cases of the **MC** and **DC2** hosts. Congruent with the observations for the **DC1**:**DAQ** system, the ESIMS data for mixtures of **5-FU** and **DC1** featured ions consistent with the presence of 1:1 and 1:2 host–guest complexes. Thus, the combined NMR and ESIMS data suggested that **DC1** can form a 1:2 host–guest complex with **5-FU**, while the **DC2** and **MC** systems can form only 1:1 adducts. A control experiment with $[Pd_2(L_{tripy})_4]^{4+}$ (where L_{tripy} = 2,6-bis(pyridin-3-ylethynyl)pyridine,[14] see Figure 1 and the Supporting Information) indicated that **5-FU** did not bind with the cavity of that simple single cage system (Supporting Information, Figure S46), consistent with the observation that **DC2** only forms a 1:1 host–guest adduct with **5-FU**.

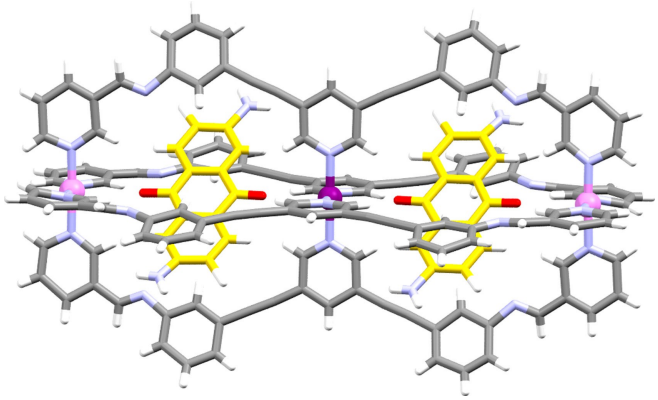

Figure 3. The molecular structure of the **DC1**:2**DAQ** host–guest complex determined using single crystal X-ray crystallography. Selected distances [Å]: Pt1–Pd1 11.733(2), Pt1–Pt1′ 23.466(2). Color: pink = platinum, purple = palladium, light blue = nitrogen, red = oxygen, grey = carbon, white = hydrogen yellow = carbon atoms of the **DAQ** guest molecules. Solvent molecules and counterions are omitted for clarity. Only one orientation for each of the disordered **DAQ** guest molecules is shown.

The interaction of **5-FU** with each of the cage systems (**MC**, **DC1** and **DC2**) was examined further using ^{1}H NMR titrations (CD_3CN, 298 K) and the corresponding data was curve-fitted using bindfit[18] to obtain the association constants (K, Supporting Information, Figures S38, S39, S41, S42, S43 and S44). For the **MC**:**5-FU** system the 1:1 binding model ($K_1 = 283 \pm 5\ M^{-1}$) provided the best fit to the titration data. Similar results were obtained with the **DC2**:**5-FU** system and the 1:1 association constant was determined to be $K_1 = 210 \pm 3\ M^{-1}$. 1:2 binding models provided the most reasonable fits to the **DC1**:**5-FU** titration data (Supporting Information, Table S2). While all the 1:2 models provided similar association constants, the statistical model seemed the best giving $K_1 = 1260 \pm 20\ M^{-1}$ and $K_2 = 315 \pm 5\ M^{-1}$.

Enzymes with multiple guest binding sites often display allosteric behavior (either positive or negative cooperativity) with the binding of the first guest causing a conformation change that affects the interaction with the second. There is growing interest in these types of host–guest interactions with metallohosts.[6,19] Related metallomacrocyclic host systems that feature two identical guest binding sites have been shown to display positive cooperativity where the binding of the first guest causes a conformation change that preorganizes the second guest binding site, leading to an enhanced host–guest interaction.[20] Presumably the observed lack of any cooperativity between the **5-FU**-**DC1** binding events reflects the rather rigid nature of the double cavity architecture. The cavities of **DC1** are already preorganized for guest binding and the complexation of the first **5-FU** guest causes little to no conformational change in the host architecture leading to the statistical, non-cooperative binding behavior.

Finally, having demonstrated that mixtures of **DC2** and **5-FU** only form a 1:1 host–guest complex ($K_1 = 210 \pm 3\ M^{-1}$) with **5-FU** bound within the Pd–Pt cavity of the architecture, we examined if the remaining empty Pd–Pd cavity could bind a second, different guest molecule. It is well established that $[Pd_2(L_{tripy})_4]^{4+}$ and related systems[14a,16b,21] can bind two molecules of cisplatin (**CP**) in acetonitrile solution. Therefore, we used ^{1}H NMR spectroscopy (CD_3CN, 298 K) to study the segregated guest binding of **5-FU** and **CP** within the two different cavities of the **DC2** cage system. The ^{1}H NMR spectra (Figure 4, and Supporting Information) showed that the addition of **5-FU** (1 eq.) to **DC2** caused a downfield shift of the *endo* α-pyridyl cage protons H_j and H_s, consistent with the guest binding within the Pt–Pd cavity of the system. **CP** (2 eq.) was added to the mixture and this

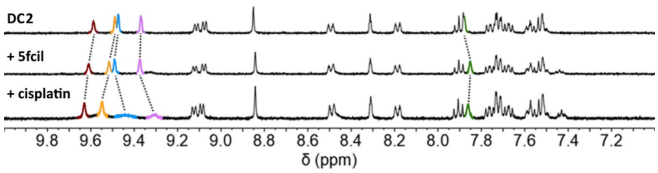

Figure 4. Stacked partial ^{1}H NMR spectra (400 MHz, CD_3CN, 298 K) of **DC2** (top), **DC2** + **5-FU** (1 eq.) (middle) and **DC2** + **5-FU** (1 eq.) and **CP** (2 eq.) complex (bottom). The proton labels correspond to those shown in Scheme 1.

caused a shift and broadening of the *endo* cage protons H_a and H_i that line the Pd–Pd cavity of **DC2**. We also examined reversing the order of the guest addition (Supporting Information, Figure S48). The addition of 2 eq. of **CP** to **DC2** caused a shift of the H_a and H_i cage proton resonances (again indicating preferential binding to the Pd–Pd cavity) and subsequent addition of **5-FU** (1 eq.) resulted in a final spectrum that was identical to that in Figure 4 (Supporting Information, Figure S48). This provides strong evidence for the selective, segregated guest binding of **CP** and **5-FU** within the two different cavities of **DC2** with the selectivity determined by the different nature of the two cages, not the order of addition.

Conclusion

We have developed a method for the assembly of the heterotrimetallic double cavity cages, $[PdPt_2L_4]^{6+}$ (**DC1**) and $[Pd_2PtL_4]^{6+}$ (**DC2**). Combining an inert platinum(II) tetrapyridylaldehyde complex with suitably substituted pyridylamine linker units and Pd^{II} ions led to the assembly of the heterotrimetallic cages through reactions facilitated by the reversible nature of imine bond formation and the relatively labile Pd-pyridyl bonds. ^{1}H and ^{1}H DOSY NMR, ESI-mass spectra and HPLC data were all consistent with the formation of the double cages. The double cages **DC1** and **DC2** displayed cavities of similar sizes to those of related homometallic $[Pd_2L_4]^{4+}$ and heterometallic cages, and the binding of a variety of different guest molecules within the double cage assemblies were studied. Heterotrimetallic $[Pd_nPt_mL_4]^{6+}$ (**DC1**) features two identical cavities and forms a host–guest adduct with two **DAQ** guest molecules, as determined by X-ray crystallography, and it also binds two molecules of the anticancer drug **5-FU**. In the latter case, the guest binding was statistical and the lack of any cooperativity between the guest binding sites was attributed to the rigid structure of the cage backbone which prevents extensive reorganization after binding the first **5-FU** molecule. **DC2** features two different cage cavities and it was shown that the two different guests, **5-FU** and **CP**, could be bound selectively within the different cavities of the double cage architecture.

Cooperativity, is commonly exploited by enzymes. Ready access to these multicavity cage structures should enable the cooperativity of molecular recognition process within these systems to be studied in more detail potentially shedding new light on how subtle factors can alter non-covalent interactions. In turn that may lead to new controllable, enzyme-like multicomponent reactions and catalysis.

Additionally, the ability to organize different guests within segregated compartments of a single discrete metallosupramolecular structure could be exploited in a range of applications, including dual guest (drug) delivery and biomimetic energy transfer processes.

Acknowledgements

L.S.L. thanks the University of Otago for a PhD Scholarship. J.D.C. thanks the University of Otago, Department of Chemistry and the MacDiarmid Institute for Advanced Materials and Nanotechnology for funding. All authors are grateful to the Marsden Fund for supporting this work (UOA1726). Open access publishing facilitated by University of Otago, as part of the Wiley - University of Otago agreement via the Council of Australian University Librarians.

Conflict of Interest

The authors declare no conflict of interest.

Data Availability Statement

The data that support the findings of this study are available in the supplementary material of this article.

Keywords: Double Cavity Cages · Heterometallic · Host–Guest Systems · Metallosupramolecular Architectures · Non-Cooperative Binding

[1] a) N. B. Debata, D. Tripathy, H. S. Sahoo, *Coord. Chem. Rev.* **2019**, *387*, 273–298; b) T. R. Cook, P. J. Stang, *Chem. Rev.* **2015**, *115*, 7001–7045; c) R. Chakrabarty, P. S. Mukherjee, P. J. Stang, *Chem. Rev.* **2011**, *111*, 6810–6918; d) H. D. Mai, N. M. Tran, H. Yoo, *Coord. Chem. Rev.* **2019**, *387*, 180–198; e) M. D. Ward, *Chem. Commun.* **2009**, 4487–4499; f) D. Zhang, T. K. Ronson, J. R. Nitschke, *Acc. Chem. Res.* **2018**, *51*, 2423–2436; g) S. Pullen, G. H. Clever, *Acc. Chem. Res.* **2018**, *51*, 3052–3064; h) S. Chakraborty, G. R. Newkome, *Chem. Soc. Rev.* **2018**, *47*, 3991–4016.

[2] a) H. Sepehrpour, W. Fu, Y. Sun, P. J. Stang, *J. Am. Chem. Soc.* **2019**, *141*, 14005–14020; b) T. R. Cook, V. Vajpayee, M. H. Lee, P. J. Stang, K.-W. Chi, *Acc. Chem. Res.* **2013**, *46*, 2464–2474; c) A. Casini, B. Woods, M. Wenzel, *Inorg. Chem.* **2017**, *56*, 14715–14729; d) A. Pöthig, A. Casini, *Theranostics* **2019**, *9*, 3150–3169; e) M. D. Ward, C. A. Hunter, N. H. Williams, *Acc. Chem. Res.* **2018**, *51*, 2073–2082; f) A. J. McConnell, C. S. Wood, P. P. Neelakandan, J. R. Nitschke, *Chem. Rev.* **2015**, *115*, 7729–7793; g) M. Yoshizawa, M. Fujita, *Bull. Chem. Soc. Jpn.* **2010**, *83*, 609–618; h) M. Yoshizawa, L. Catti, *Acc. Chem. Res.* **2019**, *52*, 2392–2404; i) M. Yoshizawa, M. Yamashina, *Chem. Lett.* **2017**, *46*, 163–171; j) V. Martí-

Centelles, A. L. Lawrence, P. J. Lusby, *J. Am. Chem. Soc.* **2018**, *140*, 2862–2868.
[3] S. Pullen, J. Tessarolo, G. H. Clever, *Chem. Sci.* **2021**, *12*, 7269–7293.
[4] a) W.-X. Gao, H.-N. Zhang, G.-X. Jin, *Coord. Chem. Rev.* **2019**, *386*, 69–84; b) H. Li, Z.-J. Yao, D. Liu, G.-X. Jin, *Coord. Chem. Rev.* **2015**, *293–294*, 139–157; c) M. Hardy, A. Lützen, *Chem. Eur. J.* **2020**, *26*, 13332–13346.
[5] R. A. S. Vasdev, D. Preston, J. D. Crowley, *Chem. Asian J.* **2017**, *12*, 2513–2523.
[6] F. J. Rizzuto, L. K. S. von Krbek, J. R. Nitschke, *Nat. Chem. Rev.* **2019**, *3*, 204–222.
[7] a) S. Bandi, S. Samantray, R. D. Chakravarthy, A. K. Pal, G. S. Hanan, D. K. Chand, *Eur. J. Inorg. Chem.* **2016**, 2816–2827; b) S. Bandi, A. K. Pal, G. S. Hanan, D. K. Chand, *Chem. Eur. J.* **2014**, *20*, 13122–13126; c) K. Yazaki, M. Akita, S. Prusty, D. K. Chand, T. Kikuchi, H. Sato, M. Yoshizawa, *Nat. Commun.* **2017**, *8*, 15914; d) R. Zhu, I. Regeni, J. J. Holstein, B. Dittrich, M. Simon, S. Prévost, M. Gradzielski, G. H. Clever, *Angew. Chem. Int. Ed.* **2018**, *57*, 13652–13656; *Angew. Chem.* **2018**, *130*, 13840–13844; e) M. D. Johnstone, E. K. Schwarze, G. H. Clever, F. M. Pfeffer, *Chem. Eur. J.* **2015**, *21*, 3948–3955.
[8] D. Preston, J. E. M. Lewis, J. D. Crowley, *J. Am. Chem. Soc.* **2017**, *139*, 2379–2386.
[9] S. Samantray, S. Krishnaswamy, D. K. Chand, *Nat. Commun.* **2020**, *11*, 880.
[10] K. Wu, B. Zhang, C. Drechsler, J. J. Holstein, G. H. Clever, *Angew. Chem. Int. Ed.* **2021**, *60*, 6403–6407; *Angew. Chem.* **2021**, *133*, 6473–6478.
[11] a) R. Zhu, J. Luebben, B. Dittrich, G. H. Clever, *Angew. Chem. Int. Ed.* **2015**, *54*, 2796–2800; *Angew. Chem.* **2015**, *127*, 2838–2842; b) S. Löffler, J. Lübben, L. Krause, D. Stalke, B. Dittrich, G. H. Clever, *J. Am. Chem. Soc.* **2015**, *137*, 1060–1063; c) S. Freye, R. Michel, D. Stalke, M. Pawliczek, H. Frauendorf, G. H. Clever, *J. Am. Chem. Soc.* **2013**, *135*, 8476–8479; d) M. Frank, J. Hey, I. Balcioglu, Y.-S. Chen, D. Stalke, T. Suenobu, S. Fukuzumi, H. Frauendorf, G. H. Clever, *Angew. Chem. Int. Ed.* **2013**, *52*, 10102–10106; *Angew. Chem.* **2013**, *125*, 10288–10293; e) M. Frank, J. M. Dieterich, S. Freye, R. A. Mata, G. H. Clever, *Dalton Trans.* **2013**, *42*, 15906–15910; f) S. Freye, J. Hey, A. Torras-Galán, D. Stalke, R. Herbst-Irmer, M. John, G. H. Clever, *Angew. Chem. Int. Ed.* **2012**, *51*, 2191–2194; *Angew. Chem.* **2012**, *124*, 2233–2237; g) R. Sekiya, M. Fukuda, R. Kuroda, *Org. Biomol. Chem.* **2017**, *15*, 4328–4335; h) R. Sekiya, M. Fukuda, R. Kuroda, *J. Am. Chem. Soc.* **2012**, *134*, 10987–10997; i) R. Sekiya, R. Kuroda, *Chem. Commun.* **2011**, *47*, 12346–12348; j) M. Fukuda, R. Sekiya, R. Kuroda, *Angew. Chem. Int. Ed.* **2008**, *47*, 706–710; *Angew. Chem.* **2008**, *120*, 718–722.
[12] L. X. Cai, D. N. Yan, P. M. Cheng, J. J. Xuan, S. C. Li, L. P. Zhou, C. B. Tian, Q. F. Sun, *J. Am. Chem. Soc.* **2021**, *143*, 2016–2024.
[13] L. S. Lisboa, J. A. Findlay, L. J. Wright, C. G. Hartinger, J. D. Crowley, *Angew. Chem. Int. Ed.* **2020**, *59*, 11101–11107; *Angew. Chem.* **2020**, *132*, 11194–11200.
[14] a) J. E. M. Lewis, E. L. Gavey, S. A. Cameron, J. D. Crowley, *Chem. Sci.* **2012**, *3*, 778–784; b) K. J. Kilpin, M. L. Gower, S. G. Telfer, G. B. Jameson, J. D. Crowley, *Inorg. Chem.* **2011**, *50*, 1123–1134.
[15] K. Sonogashira, Y. Tohda, N. Hagihara, *Tetrahedron Lett.* **1975**, *16*, 4467–4470.
[16] a) D. Preston, J. E. Barnsley, K. C. Gordon, J. D. Crowley, *J. Am. Chem. Soc.* **2016**, *138*, 10578–10585; b) D. Preston, A. Fox-Charles, W. K. C. Lo, J. D. Crowley, *Chem. Commun.* **2015**, *51*, 9042–9045.
[17] Deposition number 2129018 contain(s) the supplementary crystallographic data for this paper. These data are provided free of charge by the joint Cambridge Crystallographic Data Centre and Fachinformationszentrum Karlsruhe Access Structures service.
[18] a) D. Brynn Hibbert, P. Thordarson, *Chem. Commun.* **2016**, *52*, 12792–12805; b) P. Thordarson, *Chem. Soc. Rev.* **2011**, *40*, 1305–1323; c) http://supramolecular.org/.
[19] a) F. J. Rizzuto, J. P. Carpenter, J. R. Nitschke, *J. Am. Chem. Soc.* **2019**, *141*, 9087–9095; b) V. Martí-Centelles, R. Spicer, P. Lusby, *Chem. Sci.* **2020**, *11*, 3236–3240.
[20] a) S.-Y. Chang, H.-Y. Jang, K.-S. Jeong, *Chem. Eur. J.* **2004**, *10*, 4358–4366; b) J. D. Crowley, I. M. Steele, B. Bosnich, *Eur. J. Inorg. Chem.* **2005**, 3907–3917.
[21] A. Schmidt, V. Molano, M. Hollering, A. Poethig, A. Casini, F. E. Kuehn, *Chem. Eur. J.* **2016**, *22*, 2253–2256.

Manuscript received: January 31, 2022
Accepted manuscript online: February 22, 2022
Version of record online: March 4, 2022